2016

A Study on High Efficiency Wing-Vane Compressor - Part.2: Lubrication Characteristic of The Partial Arc Guide Bearing -

Tatsuya Sasaki
Mitsubishi Electric Corporation, Japan, sasaki.tatsuya@ea.mitsubishielectric.co.jp

Shin Sekiya
Mitsubishi Electric Corporation, Japan, sekiya.shin@eb.mitsubishielectric.co.jp

Raito Kawamura
Mitsubishi Electric Corporation, Japan, kawamura.raito@cj.mitsubishielectric.co.jp

Hideaki Maeyama
Mitsubishi Electric Corporation, Japan, maeyama.hideaki@dx.mitsubishielectric.co.jp

Shinichi Takahashi
Mitsubishi Electric Corporation, Japan, takahashi.shinichi@bk.mitsubishielectric.co.jp

See next page for additional authors

Authors
Tatsuya Sasaki, Shin Sekiya, Raito Kawamura, Hideaki Maeyama, Shinichi Takahashi, and Kanichiro Sugiura

A Study on High Efficiency Wing-Vane Compressor -Part 2: Lubrication Characteristic of The Partial Arc Guide Bearing-

Tatsuya SASAKI[1]*, Shin SEKIYA[2], Raito KAWAMURA[3], Hideaki MAEYAMA[4], Shinichi TAKAHASHI[5], Kanichiro SUGIURA[6]

[1,2,3]Mitsubishi Electric Corporation, Advanced Technology R&D Center,
8-1-1, Tsukaguchi-Honmachi, Amagasaki-City, Hyogo, Japan
Phone: +81-6-6497-7582, Fax: +81-6-6497-7285,
[1]E-mail: Sasaki.Tatsuya@ea.MitsubishiElectric.co.jp
[2]E-mail: Sekiya.Shin@eb.MitsubishiElectric.co.jp
[3]E-mail: Kawamura.Raito@cj.MitsubishiElectric.co.jp

[4]Mitsubishi Electric Corporation, Living Environment Systems Laboratory,
3-18-1, Oshika, Suruga-ku, Shizuoka-City, Shizuoka, Japan
Phone: +81-54-287-3053, Fax: +81-54-287-3056,
E-mail: Maeyama.Hideaki@dx.MitsubishiElectric.co.jp

[5,6]Mitsubishi Electric Corporation, Shizuoka Works,
3-18-1, Oshika, Suruga-ku, Shizuoka-City, Shizuoka, Japan
Phone: +81-54-287-3112, Fax: +81-54-287-3127,
[5]E-mail: Takahashi.Shinichi@bk.MitsubishiElectric.co.jp
[6]E-mail: Sugiura.Kanichiro@ay.MitsubishiElectric.co.jp

ABSTRACT

Low global warming potential refrigerants such as HFO-1234yf are attractive as alternative refrigerants in air-conditioning and cooling systems. However, larger compressor sizes were required due to the lower fluid density compared with R410A. Thus, a new wing-vane compressor which has no contact between the vane and the cylinder has been developed to prevent an increase in the size without performance degradation. The rotary motion of the vane is supported by the partial arc vane guide on the upper and lower ends of the vane. Discovering the lubrication properties of the vane guide was one of the issues required in development. So we analyzed the friction coefficient between the vane guide and the guide bearing with numerical analysis, and measured the friction coefficient by experiment. We confirmed that the friction coefficient of the analysis and experiment result are in good agreement, and can be organized in a Stribeck curve as well as full journal bearing in the fluid lubrication region.

1. INTRODUCTION

Low global warming potential refrigerants such as HFO (hydro fluoro olefin) -1234yf are attractive as alternative working fluids in air-conditioning and cooling systems to address global warming (Minor, 2008). However, larger compressor sizes were required due to the lower fluid density compared with conventional refrigerants such as R410A (Akasaka, 2010). Thus, a new wing-vane compressor which has no contact between the vane and the cylinder has been developed to prevent an increase in the size without performance degradation. The rotary motion of the vane is supported by the partial arc vane guide on the upper and lower ends of the vane. Discovering the lubricating properties of the vane guide was one of the issues required in development. So we clarified the friction

coefficient between the vane guide and the guide bearing by lubrication analysis and experiment, and evaluated the stability of the vane guide attitude by motion analysis.

2. COMPRESSOR STRUCTURE AND LUBRICATION PROBLEM

Figure 1 shows the basic structure of the wing-vane compressor. The wing-vane compressor consists chiefly of a shell, a motor, and a compression mechanism. Low pressure refrigerant taken in from the suction port is compressed to high pressure in the compression mechanism, and discharged to the refrigerant pipe after passing through the shell and the discharge port. The power of the motor is transmitted to the compression mechanism via the shaft. The vane which divides the compression chamber has a partial arc vane guide on its upper and lower ends. The vane guide slides over the guide bearing which has the same curvature radius. The vane guide is a new sliding part not found in a conventional rotary compressor, and we had to clarify the lubricating properties of the vane guide to develop the wing-vane compressor.

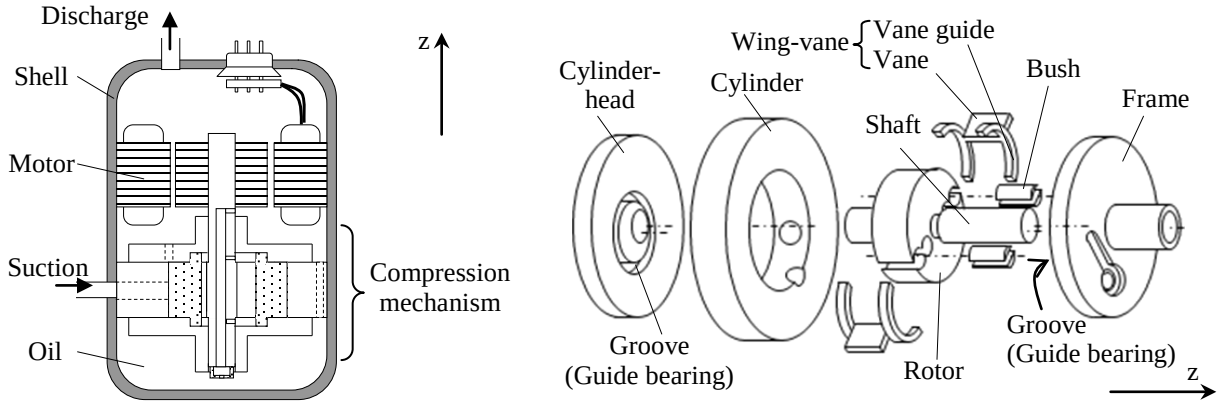

(a) Longitudinal section (b) Disassembly view of compression mechanism

Figure 1: Basic structure of wing-vane compressor

3. LUBRICATION PROPERTY OF GUIDE BEARING

We predicted the friction coefficient between the vane guide and the guide bearing by lubrication analysis with a static load. The validity of the analytical model was verified by comparing the experimentally measured friction coefficient by simulating the sliding between the vane guide and the guide bearing.

3.1 Guide Bearing Load

Figure 2 shows the calculation model of the vane guide characteristics, where F_b is a radial direction force acting on the vane due to the pressure difference between the vane back and the vane tip, and F_{cv} and F_{ca} are the centrifugal forces of vane and vane guide respectively. Here, F_p is the gas load caused by the pressure difference between the adjacent compression chambers, and F_s is bush reaction force. The result of these forces acting on the vane is applied to the vane guide, Figure 2b, where M is the vane longitudinal direction coordinate, N is the vane orthogonal direction coordinate, m is the center of the vane guide direction coordinate, and n is the coordinate at right angle to m coordinate. Here, F_m and F_n are the vane guide force of the m direction and n direction respectively. The result of F_m and F_n is represented as F. The angle of the F direction and m coordinates is defined as ϕ.

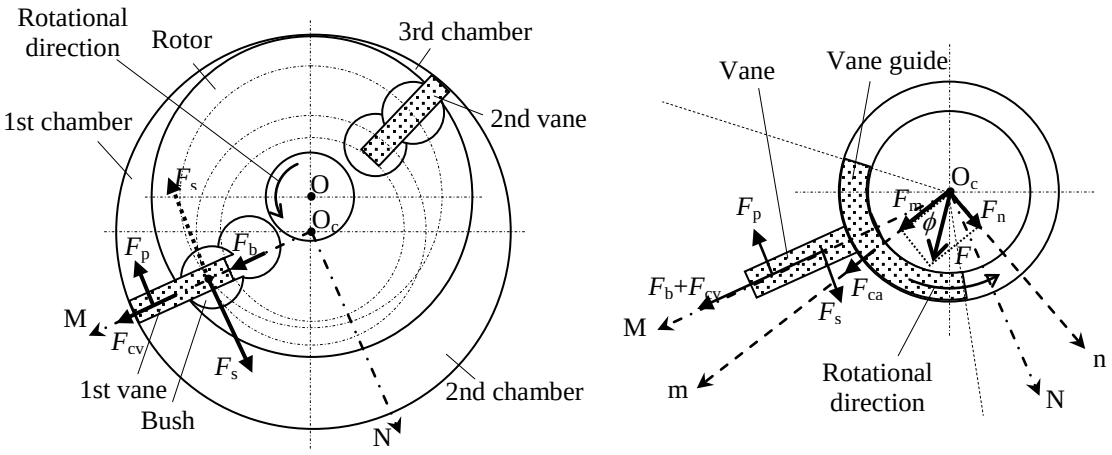

(a) Load applied on vane and bush (b) Load applied on vane guide

Figure 2: Calculation model of vane guide characteristics

3.2 Analysis Model

In order to satisfy hydrodynamic lubrication in the guide bearing, we analyzed the oil film pressure by solving the Reynolds equation of oil film between the vane guide and the guide bearing. We first considered the sliding condition of the vane guide and the guide bearing. Figure 3 shows a magnified view of around the bush. The vane moves by the rotation of the rotor through the bush. When the rotor rotates in the counterclockwise direction, the bush (a) and the vane side are in contact. A clearance is formed between the bush (b) and the vane of the opposite side. With this movement the clearance of the vane guide and the guide bearing at point B expand larger than at point A. Figure 4 is a diagram of the guide bearing which simulates the movement in Figure 3, where the Reynolds equation of oil flowing through the clearance between the vane guide and the guide bearing is expressed by Equation (1), where h is oil film thickness, p is oil film pressure, η is oil viscosity, and v_j is sliding velocity. The Reynolds equation was solved numerically by the finite difference method.

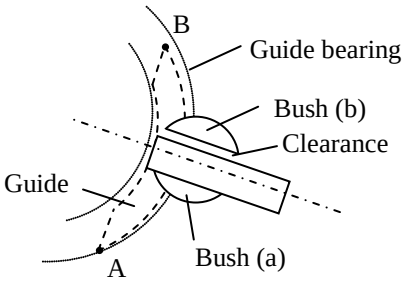

Figure 3: Magnified view of around bush

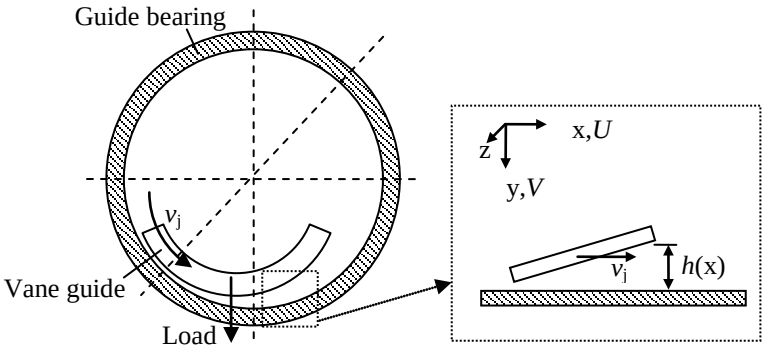

(a) Overall view (b) Magnified view of clearance

Figure 4: Diagram of guide bearing

$$\frac{\partial}{\partial x}\left(h^3\frac{\partial p}{\partial x}\right)+\frac{\partial}{\partial z}\left(h^3\frac{\partial p}{\partial z}\right)=-6\eta v_j\frac{\partial h}{\partial x} \tag{1}$$

3.3 Experiment

The friction coefficient was measured by the test apparatus simulating the sliding of the vane guide and the guide bearing in order to verify the validity of the analysis results, and the presence or absence of contact was confirmed.

3.3.1 Experimental apparatus: Figures 5 and 6 show a schematic view of the experimental apparatus and a perspective view of the test vane guide. The test apparatus has a configuration which loads and slides the test vane

guide to the rotating test guide bearing in an atmosphere. The driving force of the motor is transmitted to a spindle which drives the test guide bearing via a belt. The test vane guide is attached to the shaft through a bush. The shaft is supported by the base. When the loading shaft is strained, a load is applied to the test vane guide by the spring. The frictional force acting on the test vane guide is measured by the load cell facing the torque arm attached to the upper end of the shaft. Lubricating oil is dropped from the oil supply path of the upper end of the shaft, when the test guide bearing rotates, oil is supplied to the sliding surface by centrifugal force. To measure the temperature of the lubricating oil, thermocouples inserted in the oil supply path are fixed to the lower end of the shaft. The sliding surface roughness of the test guide bearing and the test vane guide is 0.8 μm in a ten-point average roughness. Using a contact electric resistance method, contact between the sliding surfaces was examined (Yano, 2015). The potential difference between the test vane guide and the test guide bearing was measured

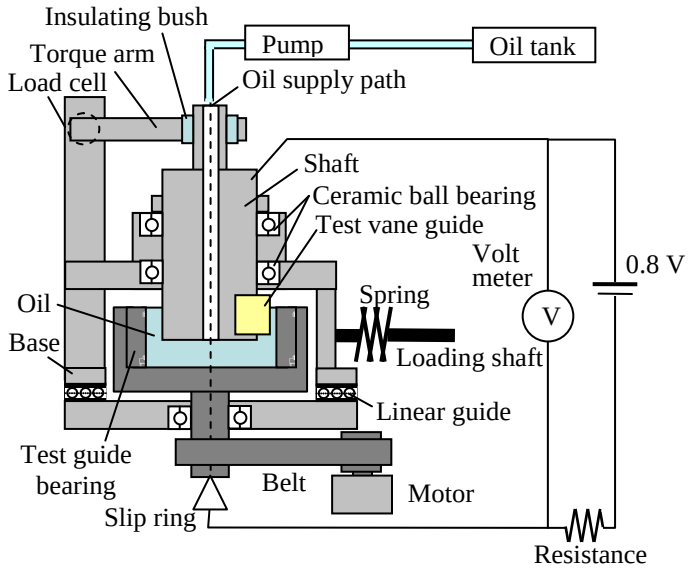

Figure 5: Schematic view of experimental apparatus

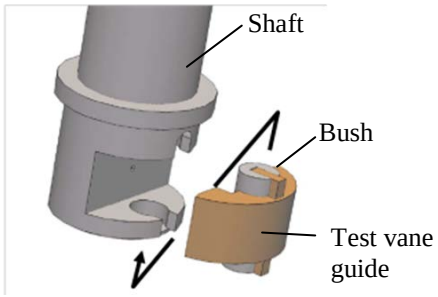

Figure 6: Perspective view of the test vane guide

3.3.2 Experimental conditions: The parameters that affect the lubricating properties of the guide bearing are the load direction, the arc angle, the load value, the viscosity of the lubricating oil, the rotational speed, the bearing radius, and the radial clearance. These parameters other than the load direction and the arc angle can be organized in a Sommerfeld number represented by Equation (2), where N_b is the rotational speed, F is the load acting on the vane guide, L is the guide bearing width, R is the guide bearing radius, and C is the radial clearance. Table 1 shows the test conditions. Figure 7 shows the load direction on the test vane guide. The load is applied in the range of 0-40 degrees toward the counter-rotation direction of the test guide bearing. The rotational speed was constant, the load was increased by 10 N up to 10-100 N, and the contact resistance and the friction coefficient were measured for 60 seconds.

$$S = 2\eta \frac{N_b}{F} LR\left(\frac{R}{C}\right)^2 \tag{2}$$

Table 1: Test conditions

Load	10-100	N
Load Direction	0-40	deg.
Rotating Speed	20	rps
Arc Angle	30-95	deg.
Sommerfeld Number	0.1-5	-
Oil Viscosity @ 313 K	3.4×10^{-3}	Pa・s

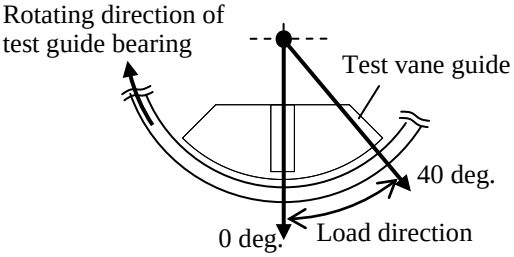

Figure 7: Load direction on the test vane guide

3.4 Analysis and Experimental Result

3.4.1 The effect of the load direction on the friction coefficient: Figure 8 shows the relationship of the friction coefficient and load direction at the arc angle of 95 degrees. In the load direction of 0 degrees, the experimental and the analytical results show a good agreement in the test range. The friction coefficient becomes lower as the Sommerfeld number becomes smaller, it can be seen that the fluid lubrication region is maintained. It was confirmed that the friction coefficient of the guide bearing is organized in a Stribeck curve in the same way as the full journal bearings. When the load direction is not less than 25 degrees, a minimum point exists on the friction coefficient in the region where the Sommerfeld number is smaller than the minimum point of the friction coefficient. With a decreasing Sommerfeld number the friction coefficient increases. Because of increasing the load the oil film thickness is reduced and the test vane guide has contact with the test guide bearing. When the load direction is 40 degrees, it is considered the oil film was broken throughout the test range. The index showing the state of surface contact is generally expressed by Equation (3), where Λ is the film thickness ratio, h is the oil film thickness, and σ is the root-mean-square roughness of each surface (Kimura, 2001). Subscripts 1 and 2 denote the guide bearing and guide.

$$\Lambda = \frac{h}{\sqrt{\sigma_1^{\,2} + \sigma_2^{\,2}}} \tag{3}$$

When the projections of the roughness are assumed to be normally distributed, it is considered that $\Lambda > 3$ in fluid lubrication region, and $\Lambda \leqq 3$ in mixed lubrication region. The roughness of the test vane guide and the test guide bearing are 0.8 μm in ten-point mean roughness. In the load direction of 30 degrees, the minimum oil film thickness is 3.5 μm, and the thickness ratio is 3.1, suggesting that it is a condition for transition from fluid lubrication region to mixed lubrication region. Figure 9 shows the results of difference in potential. When the test vane guide and the test guide bearing are separated by an oil film, the potential difference indicates equivalent to the input voltage 0.8 V. When both are in contact the voltage drops lower. When the load direction is 0 degrees, the potential difference in the tested range is constant at 0.8 V, indicating that the test guide bearing and the test vane guide are separated by an oil film. When the load direction is 25 degrees, the reduction ratio of the potential difference is increased when the Sommerfeld number is below 0.3, and it was found that this corresponds to the friction coefficient of Figure 8. When the load direction is 40 degrees, the potential difference has a low value over the entire test range, consistent with the trend of the friction coefficient.

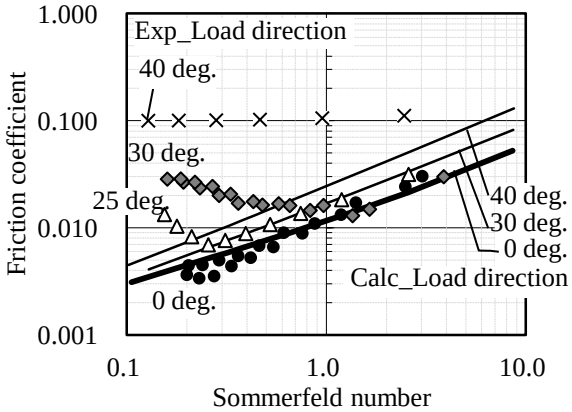

Figure 8: The relationship of friction coefficient and load direction

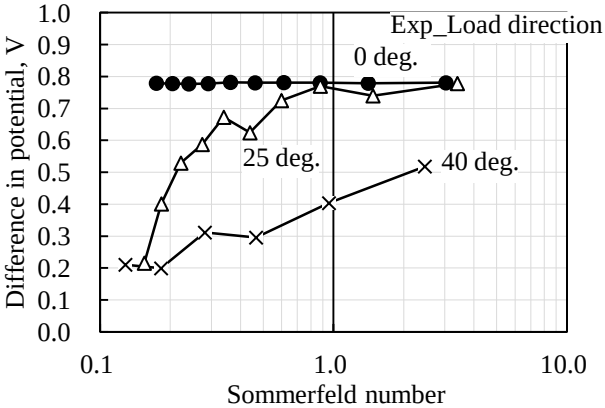

Figure 9: Result of difference in potential

3.4.2 The effect of the arc angle on the friction coefficient: Figure 10 shows the relationship of the friction coefficient and the arc angle of the guide. The load direction is constant at 0 degrees. When the arc angle is 95 degrees and 50 degrees, the friction coefficient is consistent with the analysis result. It can be seen that the sliding condition is a fluid lubrication region. When the arc angle is 40 degrees, the sliding state transited from the fluid lubrication region to the mixed lubrication region with the Sommerfeld number being smaller. When the arc angle

was 30 degrees, it was impossible to maintain the fluid lubrication state in the test range. The Sommerfeld number at the time of transition to the mixed lubrication region increases as the arc angle becomes smaller.

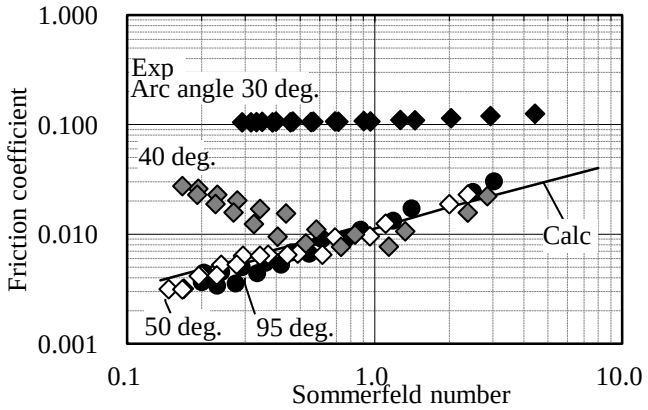

Figure 10: The relationship of arc angle of guide and friction coefficient

4. STABILITY ANALYSIS (DYNAMIC CHARACTERISTICS)

4.1 Motion Equation

During the actual operation of the compressor the load of vane guide varies in magnitude and direction. To predict the operating conditions in which the vane guide can be maintained stably, a vane guide motion analysis was conducted. Figure 11 shows the vane guide load under the low load conditions (evaporation and t condensation temperature is 308 K and 298 K respectively). Figure 12 is a diagram of the vane guide load when the load direction is on the outside of the arc angle. In the figure, the clearance between the vane guide and the guide bearing becomes a reverse wedge shape and oil film pressure does not occur. At this time, the clockwise moment *N* around point A acts on the vane guide. As the clearance between the vane guide and the guide bearing at point B expand, the frictional force acts on the bush plane and the bush cylindrical surface inhibits the separation movement of the vane guide.

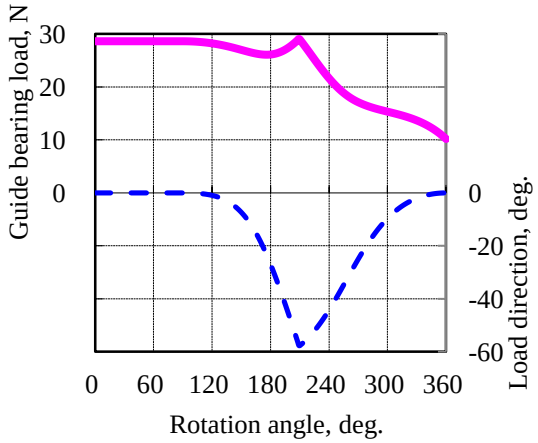

Figure 11: Vane guide load

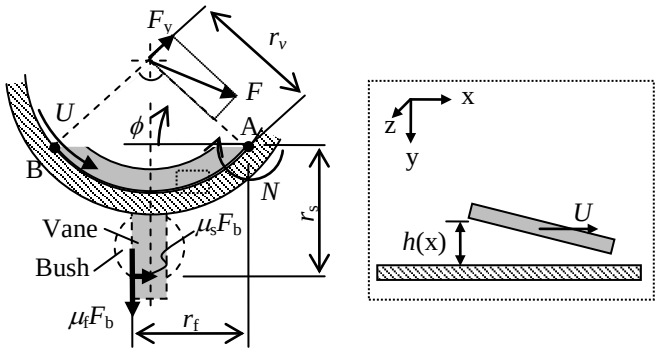

(a) Overall view (b) Magnified view of clearance

Figure 12: Diagram of vane guide load

The motion equation is expressed by Equation (4), where I is the inertia moment about point A of the vane guide, ϕ is the displacement angle around point A of the vane guide, t is time, and N is the sum of the moment. Here, ϕ is defined as 0 degrees when point B of the vane guide is in contact with the guide bearing. The moment M^+ where the vane guide is separated off from the guide bearing is expressed by Equation (5). When the vane guide starts to separate from the guide bearing the reaction force acts from the bush to the vane, friction force $\mu_f F_b$ acts between the

vane and the bush plane, the same as $\mu_s F_b$ which acts between the holder and the bush cylindrical surface, where μ_s is friction coefficient of the vane and bush plane, and μ_f is friction coefficient of the bush holder and bush cylindrical surface. Moment M^- with these forces is expressed by Equation (6). The length of the moment arm is represented by r_v, r_f, r_s. In addition, the derivative term of Equation (4) is represented as shown in Equation (7), where ω is the angular velocity of the vane guide movement direction. Moment N is the sum of Equations (5) and (6), and Equation (8) is obtained by substituting Equations (5)-(7) in Equation (4). Since F_y and F_b are a function of time they can be represented as $F_y = F_y(t)$, $F_b = F_b(t)$. Further, dimensionless $\bar{t}$ and $\bar{\omega}$ are represented by Equations (9) and (10), where ω_v is the angular velocity of the vane guide along the guide bearing. Equation (11) is obtained by substituting Equations (9) and (10) into Equation (8). Equations (12) and (13) are obtained by integrating Equation (11) twice. Since solving the integral calculation analytically is difficult, the dimensionless angular velocity and the displacement angle are calculated with the Riemann integral shown in Equations (12) and (13).

$$I\frac{d^2\phi}{dt^2} = N \tag{4}$$

$$M^+ = F_y r_v \tag{5}$$

$$M^- = -\mu_f F_b r_f - \mu_s F_b r_s \tag{6}$$

$$\frac{d^2\phi}{dt^2} = \frac{d\omega}{dt} \tag{7}$$

$$\frac{d}{dt}\omega = \frac{1}{I}\left(F_y r_v - \mu_f F_b r_f - \mu_s F_b r_s\right) \tag{8}$$

$$\bar{t} = \omega_v t \tag{9}$$

$$\bar{\omega} = \frac{\omega}{\omega_v} \tag{10}$$

$$\frac{d\bar{\omega}}{d\bar{t}} = \frac{1}{I\omega_v^2}\left\{r_v F_y(\bar{t}) - \left(\mu_f r_f + \mu_s r_s\right)F_b(\bar{t})\right\} \tag{11}$$

$$\bar{\omega} = \frac{1}{I\omega_v^2}\int\left\{r_v F_y(\bar{t}) - \left(\mu_f r_f + \mu_s r_s\right)F_b(\bar{t})\right\}d\bar{t} \tag{12}$$

$$\phi = \frac{1}{I\omega_v^2}\int\int\left\{r_v F_y(\bar{t}) - \left(\mu_f r_f + \mu_s r_s\right)F_b(\bar{t})\right\}d\bar{t}d\bar{t} \tag{13}$$

4.2 Analysis Conditions

Table 2 shows the analysis conditions. So that the load direction was outside of the vane guide arc, we set the guide arc angle to 50 degrees. As shown in Figure 11 the vane guide become unstable statically under the low load conditions(evaporation and condensation temperature is 308 K and 298 K respectively) when the load direction is outside of the vane guide arc in the rotational angle range of 178-269 degrees.

Table 2: Analysis conditions

Rotating speed	20	rps
Arc angle of guide	50	deg.
Friction coefficient of bush	Variable	-

4.3 Analysis Result

Figure 13 shows the analysis results. It shows a separation range analyzed by the static analysis in the figure too. The separation range becomes narrow as the friction coefficient of bush becomes large. With a bush friction

coefficient of 0.1, it was found that separation of the vane guide from the guide bearing was suppressed. In conditions where the load direction becomes outside of the vane guide arc, as the friction coefficient of the bush increase, the stability of the vane improves. The actual compressor verification results are reported in Part 3.

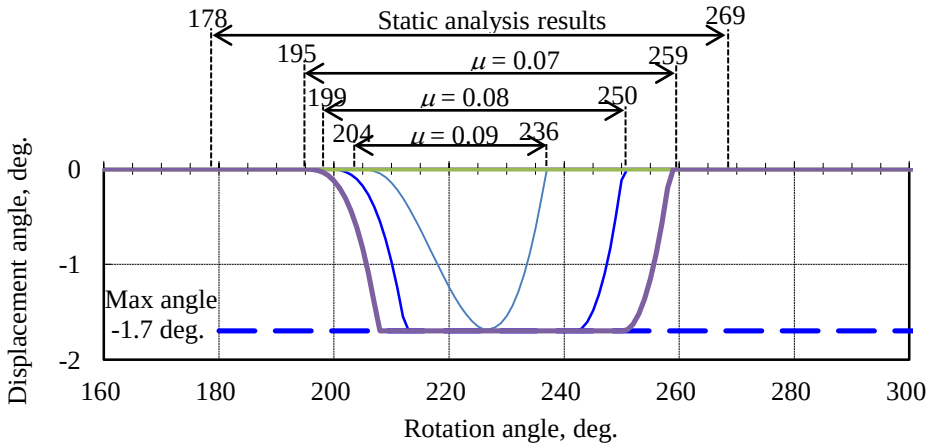

Figure 13: Analysis results

5. CONCLUSIONS

To establish a design technology for the guide bearing which is specific to the wing-vane compressor, the static lubricating analysis of the guide bearing was considered and compared to the friction coefficient by experiment. It was subjected to motion analysis in consideration of the fluctuating load to clarify the behavior and lubrication performance of the guide bearing in the region where the load direction is out of the vane guide arc and the oil film pressure does not occur. The results are shown below.

- When the load acts on the center of the arc angle of the vane guide, the analysis results and the test results of the friction coefficient match and it is revealed that lubrication analysis of guide bearing according static load is appropriate.
- If the guide bearing is satisfied by fluid lubrication region, the friction coefficient can be organized in a Stribeck curve as well as full journal bearings.
- When the load direction is equal to or larger than 25 degrees, lubrication condition changes from fluid lubrication region to mixed lubrication region as the Sommerfeld number is reduced, and as the load direction is large the Sommerfeld number at the boundary of mixed lubrication region and fluid lubrication region is large.
- Where the arc angle of the vane guide is small, the lubrication state is likely to transition from fluid lubrication region to mixed lubrication region.
- As a result of motion analysis it was revealed that the displacement of the vane guide can be reduced by considering the frictional force of the bush in the region where the load direction is out of the vane guide arc.

REFERENCES

Barbara, M., & Mark, S. (2008). HFO-1234yf low GWP refrigerant update. *International Refrigeration and Air Conditioning Conference at Purdue* (2349). Indianapolis, IN: Purdue University.

Ryo, A., Yohei, K., Katsuyuki, T., & Yukihiro, H. (2010). *JSRAE Thermodynamic Table Vol.3 HFO-1234yf*. Japan: Japan Society of Refrigerating and Air Conditioning Engineers.

Akihiko, Y., Eiichi, I., Masaki, M., & Sadao, Y. (2015). Study on the load carring of sliding bearing lubricated by synthetic ester oils, *Tribology Online*, *10*(5), 377-389.

Yoshitsugu, K. (2001). *Tribology Handbook*. Japan: Yokendo.